Genes: Structure and Regulation:

Regulation of *Drosophila* Hypoxia-inducible Factor (HIF) Activity in SL2 Cells: IDENTIFICATION OF A HYPOXIA-INDUCED VARIANT ISOFORM OF THE HIFα HOMOLOG GENE similar

Thomas A. Gorr, Takeshi Tomita, Pablo Wappner and H. Franklin Bunn

J. Biol. Chem. 2004, 279:36048-36058.
doi: 10.1074/jbc.M405077200 originally published online May 28, 2004

THE JOURNAL OF BIOLOGICAL CHEMISTRY
Vol. 279, No. 34, Issue of August 20, pp. 36048–36058, 2004
Printed in U.S.A.

Regulation of *Drosophila* Hypoxia-inducible Factor (HIF) Activity in SL2 Cells

IDENTIFICATION OF A HYPOXIA-INDUCED VARIANT ISOFORM OF THE HIFα HOMOLOG GENE *similar*[*] [S]

Received for publication, May 7, 2004, and in revised form, May 26, 2004
Published, JBC Papers in Press, May 28, 2004, DOI 10.1074/jbc.M405077200

Thomas A. Gorr‡, Takeshi Tomita‡§, Pablo Wappner¶‖, and H. Franklin Bunn‡

From the ‡Division of Hematology, Department of Medicine, Brigham and Women's Hospital, Harvard Medical School, Boston, Massachusetts 02115 and the ¶Instituto Leloir, Consejo Nacional de Investigaciones Científicas y Técnicas, Facultad de Ciencias Exactas y Naturales, Universidad de Buenos Aires, Patricias Argentinas 435, Buenos Aires 1405, Argentina

Although hypoxia-inducible factor-α (HIFα) subunit-specific hydroxylation and proteolytic breakdown explain the binary switch between the presence (hypoxia) and absence (normoxia) of HIFs, little is known of the mechanisms that fine-tune HIF activity under constant, rather than changing, oxygen tensions. Here, we report that the *Drosophila* HIFα homolog, the basic helix-loop-helix/PAS protein Sima (Similar), in hypoxic cultures of SL2 cells is expressed in full-length (fl) and splice variant (sv) isoforms. The following evidence supports the role of flSima as functional HIFα and the role of SL2 HIF as a transcriptional activator or suppressor. The pO_2 dependence of Sima abundance matched that of HIF activity. HIF-dependent changes in candidate target gene expression were detected through variously effective stimuli: hypoxia (strong) > iron chelation, *e.g.* desferrioxamine (moderate) ≫ transition metals, *e.g.* cobalt ≃ normoxia (ineffective). Sima overexpression augmented hypoxic induction or suppression of different targets. In addition to the full-length exon 1–12 transcript yielding the 1510-amino acid HIFα homolog, the *sima* gene also expressed, specifically under hypoxia, an exon 1–7/12 splice variant, which translated into a 426-amino acid Sima truncation termed svSima. svSima contains basic helix-loop-helix and PAS sequences identical to those of flSima, but, because of deletion of exons 8–11, lacks the oxygen-dependent degradation domain and nuclear localization signals. Overexpressed svSima failed to transactivate reporter genes. However, it attenuated HIF (Sima·Tango)-stimulated reporter expression in a dose-dependent manner. Thus, svSima has the potential to regulate *Drosophila* HIF function under steady and hypoxic pO_2 by creating a cytosolic sink for the Sima partner protein Tango.

Oxygen homeostasis depends upon sensing variations in oxygen tension (pO_2) and signal transduction, leading to physiologically appropriate changes in gene expression. Virtually all aerobic prokaryotes and eukaryotes have evolved various mechanisms for regulating genes during times of oxygen deprivation (1). Particularly in hypoxia-tolerant species, *i.e.* those capable of surviving and even thriving in environments with little (hypoxia) or no (anoxia) oxygen present, these changes in gene expression, together with drastically reduced steady-state ATP levels, are critical determinants of the resilience of the organism to low oxygen (2). In contrast to most endothermic vertebrates (birds and mammals), invertebrates are often hypoxia-tolerant (3–5). For example, embryos and adult stages of the fruit fly *Drosophila melanogaster* possess a rich and varied repertoire of survival strategies endowing them to withstand and fully recover from even hour-long exposure to anoxia (N_2 atmosphere) (6). These responses vary once oxygen levels have declined to 1.6–3%, the critical pO_2 of the species (7, 8), below which insect respiration generally ceases to be regulated (9, 10). The following strategies are employed by fruit fly embryos and adults when faced with hypoxic/anoxic challenges: (*a*) ability to sense falling pO_2 within seconds via a nitric oxide signaling pathway (11), (*b*) anoxic stupor ranging from loss of coordination to complete immobility throughout the entire period of O_2 deprivation (7, 12), (*c*) greatly reduced O_2 consumption down to 20% of normoxic values (6, 12), (*d*) glycogen-fueled anaerobiosis with lactate as the major end product (5, 13), (*e*) general and reversible chromatin condensation (14), and (*f*) cell cycle arrest (11, 14–16). Another important oxygen-sensitive response in insects is the long known hypoxic stimulation of outgrowth and proliferation of tracheal termini for improved supply of limiting amounts of O_2 to tissues (17–20). This hypoxia-induced ramification of insect breathing tubes poses intriguing parallels to the O_2 response in mammalian angiogenesis (21–23).

A wide range of animals, from mammals to fruit flies to nematodes, share a common pathway that links sensing of changes in pO_2 to transcriptional regulation. Central to hypoxia-mediated gene expression are hypoxia-inducible (transcription) factors (HIFs)[1] (24–26), which belong to the family of basic helix-loop-helix (bHLH)/PAS (Per/ARNT/Sim) transcription factors (27–29). In mammals (30, 31), *Caenorhabditis elegans* (32, 33), and *Drosophila* (34–37), HIF is a heterodimer of α- and β-subunits that specifically recognizes

* This work was supported in part by National Institutes of Health Grant R01 DK41234. The costs of publication of this article were defrayed in part by the payment of page charges. This article must therefore be hereby marked "*advertisement*" in accordance with 18 U.S.C. Section 1734 solely to indicate this fact.

[S] The on-line version of this article (available at http://www.jbc.org) contains Supplemental Fig. 1 and Supplemental Table 1.

§ Supported by the Uehara Memorial Foundation.

‖ Career Investigator of the Consejo Nacional de Investigaciones Científicas y Técnicas.

** To whom correspondence should be addressed: Div. of Hematology, Dept. of Medicine, Brigham and Women's Hospital, Harvard Medical School, 221 Longwood Ave., Boston, MA 02115. Tel.: 617-732-5841; Fax: 617-739-0748; E-mail: hfbunn@rics.bwh.harvard.edu.

[1] The abbreviations used are: HIF, hypoxia-inducible factor; bHLH, basic helix-loop-helix; HRE, hypoxia response element; ODD, oxygen-dependent degradation domain; ARNT, aryl hydrocarbon receptor nuclear translocator; DFO, desferrioxamine; RT, reverse transcription; ORF, open reading frame; UTR, untranslated region; EMSA, electrophoretic mobility shift assay; svSima, splice variant Sima; flSima, full-length Sima.

short *cis*-regulatory E-box motifs called hypoxia response elements (HREs) in the promoter and/or enhancer regions of a number of genes (38, 39). Functional HREs, *i.e.* those capable of oxygen-dependent binding of HIF proteins *in vitro* and transactivating reporter genes *in vivo*, can be summarized in the following consensus sequence: 5′-*B*(A/G)CGT-G*V*BBB-3′ (where *B* is all bases except A and *V* is all bases except T) (40). The central 4-base core (underlined) is critical for the binding of any HIF complex, be it mammalian, insect, or crustacean (see accompanying article (87)).

Oxygen-dependent activation of HIF is, in cell culture, controlled primarily at the protein level through specific oxidative modifications of the α-subunit (41). The HIF oxygen sensor is a novel prolyl hydroxylase (42–44) that catalyzes the O_2-dependent hydroxylation of proline residues within the oxygen-dependent degradation domain (ODD) of HIF-1α (45). Once hydroxylated, HIF-1α binds rapidly to the von Hippel-Lindau tumor suppressor product, enabling ubiquitination and rapid degradation by the proteasome (46–49). Conversely, hypoxia and hypoxia-mimicking agents such as transition metals (*e.g.* Co^{2+}) and iron chelators (*e.g.* desferrioxamine) (42) inhibit proline hydroxylation of HIF-1α, thus enabling the protein to escape proteolytic degradation and to dimerize with HIF-1β (ARNT). The HIF dimer then translocates into the nucleus, where it activates target genes containing HRE-binding sites. This scheme for activation of HIF extends from mammals to invertebrates (42, 44). In contrast, little is known about the means utilized by *hypoxic* cells to regulate HIF function.

In *D. melanogaster*, hypoxia-specific HIF-like DNA-binding activity was first demonstrated in so-called SL2 cells cultured from late embryos of the fruit fly (50). Subsequently, structural homologs of HIF subunits were cloned in the form of the bHLH/PAS proteins Sima (Similar; HIF-1α homolog) (34) and Tango (*Drosophila* ARNT; HIF-1β homolog) (Refs. 35–37; see Ref. 27 for review). As expected for HIF proteins, Sima and Tango transcripts are ubiquitously expressed throughout embryogenesis and in nearly all tissues of *Drosophila* (34, 36). Moreover, as in mammals, Sima stability and *Drosophila* HIF activity seem to be regulated in an O_2-dependent fashion. Functionality of homologous amino acid motifs in Sima, predicted to confer normoxic instability (51), was confirmed by hypoxic inductions of luciferase reporter plasmids through Sima-Gal4 fusion constructs (52). The fact that this transactivation was observed in mammalian cells indicates that Sima is able to functionally substitute for human HIF-1α and provides evidence for the close conservation of these signaling pathways between mammals and insects. Recent work on transgenic flies by Lavista-Llanos *et al.* (53) showed that *in vivo* HIF activity is most pronounced in developing tracheal cells, wherein proliferation is hypoxia-stimulated (see above). Both Sima and Tango are absolutely required for regulating the transcription of HRE-reporter constructs within tracheae of hypoxic fly embryos.

Other α-like bHLH/PAS proteins known to also heterodimerize with Tango in a tissue-specific manner (54) were unable to elicit this hypoxic response (53). These include the neurogenic factor Sim (Single-minded) (55) and, most notably, Trh (Trachealess), the master regulator that drives early tracheal development (56, 57). Ss (Spineless), the *Drosophila* aryl hydrocarbon receptor homolog, and Dys (Dysfusion), another tracheogenetic bHLH/PAS factor, are two additional partner proteins for Tango (58, 59). Therefore, Tango can form functional heterodimers with five partners: Sima, Sim, Trh, Ss, and Dys. This growing list of Tango heterodimers with close or even overlapping DNA specificities (40, 58, 60–62) begs the question as to how, in the face of potential competition for Tango (36, 54, 59) and/or binding site interference (59) by coexpressed Tango partners, the signaling pathways mediated by each α-like bHLH/PAS protein are maintained and controlled.

To address the control and maintenance of *Drosophila* HIF signaling, we utilized SL2 cells (Schneider cells, line 2), which were originally cultured from late 20–24-h-old *Drosophila* embryos (63), a time of maximal HIF activity during *Drosophila* development (53). The fact that Sim and Trh, potential Tango competitors, are not expressed in this cell line (36) makes our investigations less complicated. Thus, SL2 cells are well suited as a model for investigating the function and control of *Drosophila* HIF.

MATERIALS AND METHODS

Cell Culture—SL2 cells were purchased from American Type Culture Collection (CRL-1963) or received as generous gifts from Drs. A. Michelson and N. Perrimon. The cells were cultured as described in the accompanying article (87). SL2 cells were grown at 22 °C in air either as monolayer or suspension cultures. Standard hypoxic challenge comprised 16-h exposure at 22 °C to 1 or 4% oxygen (balance N_2) using an Espec BNP-210 incubator (Tabai Espec Corp.). Hypoxic exposures that differed from these standard conditions are specified below. In addition, SL2 cells were exposed for 16 h to each of the known mammalian HIF-stabilizing agents $CoCl_2$ and desferrioxamine (DFO) at 100 μM (42, 64). Efforts were made to use mid-log cells for all experiments (see below).

RNA Isolation, Northern Blotting, and Reverse Transcription (RT)-PCR Experiments—Total RNA was isolated from normoxic, hypoxic (1 and 4% pO_2), cobalt-treated, or DFO-treated SL2 cells using TRIzol (Invitrogen) following the manufacturer's protocol. 25-μg aliquots of RNA were size-separated on denaturing 6% formaldehyde and 1% agarose gels, in which the 18 S rRNA and the processed half-molecules of the 28 S rRNA (*i.e.* 28 Sa and 28 Sb) (65, 66) migrated as one major band between 1.7 and 2 kb in size. Next, RNA was blotted in 20× SSC buffer onto positively charged nylon membranes (GeneScreen Plus, PerkinElmer Life Sciences) and hybridized for 16 h at 42 °C with 20–30 ng of the following RT-PCR-isolated and ^{32}P-labeled cDNA probes: (*a*) Similar (FlyBase symbol Sima and ID FBgn0015542), a 531-bp KpnI/SacI fragment between exons 1 and 3 (amino acid 1–174); (*b*) Tango (FlyBase symbol Tgo and ID FBgn0015014), 670-bp PstI fragment between amino acids 43 and 267 (the *tango* gene contains an intronless open reading frame (ORF)); (*c*) ribosomal protein L29 (FlyBase symbol RpL29 and ID FBgn0016726), 256 bp of the entire ORF; (*d*) globin-1 (FlyBase symbol Glob1 and ID FBgn0027657), 477 bp of the entire ORF; (*e*) lactate dehydrogenase (FlyBase symbol ImpL3 and ID FBgn0001258), 514-bp ClaI/BamHI fragment between exons 1 and 2 (amino acid 51–224); (*f*) CG11652 (ID FBgn0036194), 624-bp XbaI/EcoRI fragment between exons 1 and 2 (amino acids 244–454 = C terminus); and (*g*) DNA (cytosine 5)-methyltransferase-2 (FlyBase symbol Mt2 and ID FBgn0028707), a 785-bp BtgI fragment between amino acids 36 and 299 (the *mt2* gene contains an intronless ORF). Membranes were washed the following day with 0.1× SSC and 0.1% SDS solution at 55 °C and exposed to phosphoimager screens. Following stripping of the membranes, the loading control was assessed through the constitutive expression of the *rpL29* gene, which encodes a structural polypeptide of the large (60 S) ribosomal subunit. Relative changes in expression between normoxic (control) and hypoxic or hypoxia-mimicking (Co^{2+}, DFO) (64) conditions were quantified by background-subtracted object-average densitometry of the signal bands (ImageQuant Mac Version 1.2 software, Amersham Biosciences).

For RT-PCR experiments, first strand cDNA templates, derived from normoxia/hypoxia/cobalt/DFO-treated total RNAs, were amplified using gene-specific primers that mostly spanned from the 5′-untranslated region (UTR) sequences across the ATG start codon into the ORF (forward primer) and from the ORF across the stop codon into the 3′-UTR nucleotides (reverse primer) (see Supplemental Table 1 for compilation of all primers used in this study). A typical PCR protocol used Ex*Taq* polymerase (PanVera) and continued for 30 cycles at 94 °C for 1 min, 55 °C for 1 min, and 72 °C for up to 4 min. PCR products were TA-cloned into the pCR2.1/Topo cloning vector (Invitrogen) and sequenced for validation. Empirical determination of the formation of normoxic and hypoxic PCR products after various numbers of cycles helped define the exponential amplification phase for each cDNA individually. This approach was used as a second screen to monitor differential gene expression and will be referred to as RT-PCR_{exp}. In general, RT-PCR_{exp} yielded relative expression levels in excellent agreement with Northern data, yet with greater sensitivity.

Nuclear Extracts and Electrophoretic Mobility Shift Assay (EMSA)—Following 16-h exposures to normoxic, various hypoxic (0–10% oxygen), cobalt, or DFO treatments, SL2 nuclear and cytosolic extracts were prepared and used in EMSAs as described in the accompanying article (87). We used the following wild-type HRE oligonucleotide (W18) of the 3′-enhancer of the human erythropoietin gene (67) as a double-stranded ^{32}P-labeled probe and as an unlabeled competitor for all EMSA experiments reported herein: 5′-AGCTTGCCC(TACGTGCT)GTCTCAG-3′ (where the HRE is in parentheses and the core bases essential for HIF binding are underlined; only the sense strand is given). A large excess of the following M18 mutant oligonucleotide (0.75–1.5 μg) was also used in these binding reactions to minimize nonspecific (but not HIF) binding to the W18 probe: 5′-AGCTTGCCC(TAAAAGCT)GTCTCAG-3′ (where the mutated core bases are underlined).

Cloning of Full-length and Splice Variant Sima cDNAs into pAc5.1—Dr. S. Crews kindly donated a pAc5/Tango expression construct containing the full-length 1.9-kb cDNA (start-to-stop codon) of the *Drosophila tango* gene. Overexpression and cotransfection experiments of *Drosophila* HIF necessitated the cloning of the bHLH/PAS protein Sima as the functional fly HIFα homolog (52, 53). Well suited for the expression in SL2 cells, the pAc5 plasmid (version A used here; Invitrogen) contains the 2.5-kb promoter of the *Drosophila actin 5C* gene upstream of the polylinker region for high level constitutive expression of the inserted gene of interest (68). Also, upon removal of endogenous stop codons, pAc5.1 proteins are expressed with C-terminal tags in the form of poly-His sequences and the viral protein-derived V5 epitope (69), allowing for easy product detection using a commercially available anti-V5 antibody (Invitrogen).

An ~4.5-kb amplicon was obtained in Sima RT-PCRs by using a start codon-spanning forward primer (Sima-F) and a stop codon-spanning reverse primer (Sima-C_T) (Supplemental Table 1). The forward primer had a KpnI site and the reverse primer an XbaI site (in replacement of the endogenous stop codon) added to their respective 5′-ends. In these RT-PCR experiments, an ~2-kb product was consistently co-amplified using the same primers, whereas additional amplicons at ~1.2 and ~3.3 kb were only irregularly observed. The 2- and 4.5-kb products were both initially cloned into the pCR2.1/Topo vector and sequenced to completion using exon-specific forward and reverse primers (Supplemental Table 1). The 4.5-kb cloned PCR product contained the full-length start-to-stop codon cDNA of the *sima* gene composed of exons 1–12. It was ligated into the KpnI/XbaI sites of pAc5.1 in the form of two PCR artifact-free (*i.e.* no premature stop codons) subfragments from different pCR2.1 precursor clones, thus generating the expression construct pAc5.1/Sima.

On the other hand, the 2-kb product represented an exon 1–7/12 splice variant of the *sima* gene. Fusion of exons 7 and 12 resulted in a frame-shifted exon 12 translation frame. A new reverse PCR primer was generated (Sima2-C_T) (Supplemental Table 1) that spanned the exon 7–12 junction, including the first 19 nucleotides of exon 12, and that replaced the following consecutive stop codons, which resulted from the frame-shift, with an XbaI site for cloning. Together with the forward primer Sima-F, Sima2-C_T was used to amplify the 1.3-kb translation frame of the splice variant Sima (svSima) product from 2-kb exon 1–7/12 pCR2.1 precursor templates. Following a KpnI/XbaI double digestion, 1.3 kb-PCR products were inserted into these sites of pAc5.1, generating the pAc5.1/svSima construct.

Western Blotting—25 μg of nuclear or cytosolic protein extracts (see "Nuclear Extracts and Electrophoretic Mobility Shift Assay (EMSA)" above), obtained from non-transfected or mock-, pAc5.1/Sima-, pAc5/Tango-, or pAc5.1/svSima-transfected normoxic and hypoxic SL2 cells, was loaded per lane onto 8% SDS-polyacrylamide gels and size-separated. Thereafter, proteins were blotted onto Hybond ECL nitrocellulose membranes (Amersham Biosciences), and membrane surfaces were coated with suspensions of 5% milk and Tris-buffered saline/Tween 20. Antibody labeling took place during overnight incubations at 4 °C using (*a*) 1:1000 dilutions of rat anti-Sima antiserum, (*b*) 1:1000 dilutions of mouse anti-Tango monoclonal antibody (generous gift of Dr. S. Crews), or (*c*) 1:5000 dilutions of horseradish peroxidase-conjugated mouse anti-V5 monoclonal antibody (Invitrogen). Following labeling with horseradish peroxidase-conjugated anti-rat (for Sima) or anti-mouse (for Tango) IgG secondary antibodies, all immunoblots were developed by ECL and exposed to ECL Hyperfilm (Amersham Biosciences).

SL2 Cotransfections—Cotransfections of SL2 cells (10 ml at 0.5×10^6 cells/ml) were conducted using a calcium phosphate kit (Invitrogen) following the manufacturer's recommendations (70, 71). Cells were transfected for 16 h with a total of 22.5 μg of DNA using the pUC18 plasmid as filler DNA where necessary. This amount of DNA included 1 μg of HRE-luciferase reporter, 0.25 μg of pAc5.1/*lacZ* plasmid for normalization of luciferase activities to varying transfection efficiencies, 0.25 μg of HIF expression plasmids (*i.e.* pAc5.1/Sima, pAc5/Tango, pAc5.1/svSima), and 0.65–6.5 μg of pAc5.1/svSima plasmid in titration experiments (see below). To generate a suitable HRE-luciferase reporter, a −462 base deletion product of the promoter of the hypoxia-inducible hemoglobin-2 gene from the freshwater crustacean *Daphnia magna*, housing three HREs at positions −258, −146, and −107, two of which are able to bind human, *Drosophila*, or *Daphnia* HIF complexes (see accompanying article (87)), was cloned into the KpnI/MluI sites upstream of the luciferase gene in the pGL3-Basic luciferase plasmid (Promega) (denoted by HRE in Fig. 7). A 1:4 (0.25:1 μg) ratio between expression and reporter plasmids was adopted to obtain maximal hypoxically induced transactivations of the luciferase gene as seen in pilot transfections. Negative controls included plasmid-free and insert/HRE-free pGL3-Basic luciferase vector-only transfections. After transfection, culture of washed cells was continued in new medium for another 48 h. Halfway through this period, transfected cultures were split into two equal size populations for parallel normoxic (21% pO_2 at 22 °C) *versus* hypoxic (1% pO_2 at 22 °C) exposures, which occupied the final 16 h prior to harvest. Normalized luciferase activities (*i.e.* luciferase/β-galactosidase activity ratios) are expressed as a percentage of the total sum of all normoxic and hypoxic activities, with the hypoxic/normoxic activity ratio expressed as -fold hypoxic induction.

RESULTS AND DISCUSSION

To initiate our investigation of the identity of SL2 HIF components, Northern blot and RT-PCR experiments were carried out to test the expression of the following bHLH/PAS transcription factors in Schneider cells: Sima, Sim, Trh, Dys, and Ss as HIF α-like subunit proteins (29) and Tgo (*Drosophila* ARNT) as a HIF β-like subunit protein (Fig. 1*a*). Although Sim and Trh, in agreement with earlier reports (36), and Ss were not expressed in SL2 cells, the Dys transcript was successfully amplified using RT-PCR (data not shown). Additionally, the Northern blot in Fig. 1*b* demonstrates abundant and constitutive expression of Sima and Tango, regardless of different conditions: exposure to normoxia, hypoxia (1 and 4% oxygen), or hypoxia mimetics (cobalt or desferrioxamine). The constitutive expression of Sima and Tango mRNAs in Fig. 1*b* suggests that HIF in *Drosophila*, as in mammals, is regulated by a post-transcriptional control mechanism involving the oxygen-dependent stability of the α-subunit. Of all *Drosophila* HIFα candidates (Fig. 1*a*), the Sima protein uniquely contains an ODD-like region including a highly conserved sequence around proline 850 (51) as a potential hydroxylation target (Fig. 1*c*). For this reason, we sought to assess the activity of *Drosophila* HIF along with the stability of the α-subunit candidate Sima as a function of pO_2.

Fig. 2*a* shows a typical gel shift experiment using an HRE probe (W18) derived from the human erythropoietin enhancer (67) along with nuclear extracts from normoxic (21% pO_2; *lane 2*) or hypoxic (1% pO_2; *lanes 3* and *4*) Schneider cells. SL2 HIF was found to be represented by two retarded bands (*black* and *white arrows*) that showed a marked increase in activity in hypoxic extracts (*lane 3 versus lane 2*). The binding specificity of *Drosophila* HIF to the human erythropoietin enhancer W18 probe is demonstrated in *lane 4*, where addition of 100-fold excess unlabeled competitor probe resulted in the disappearance of both bands. Following a 16-h exposure of mid-log phase SL2 cells to different oxygen tensions, maximal HIF activity was detected at 1% oxygen, with progressively declining activity levels toward both anoxia and higher oxygen tensions (negligible activity at $pO_2 \geq 10\%$) (Fig. 2*b*). At $pO_2 \geq 1\%$, a double-banded gel shift was observed (*lanes 3–5*, *black* and *white arrows*), whereas nuclear extracts from <1% pO_2 incubations consistently contained only the lesser mobility complex (*lanes 1* and *2*, *black arrow*). Thus, SL2 HIF can assemble into different complexes in an oxygen-dependent manner. Phosphoimaging densitometry of the top complex showed that mean SL2 HIF activities were maximal at 1% oxygen (~4-fold induced relative

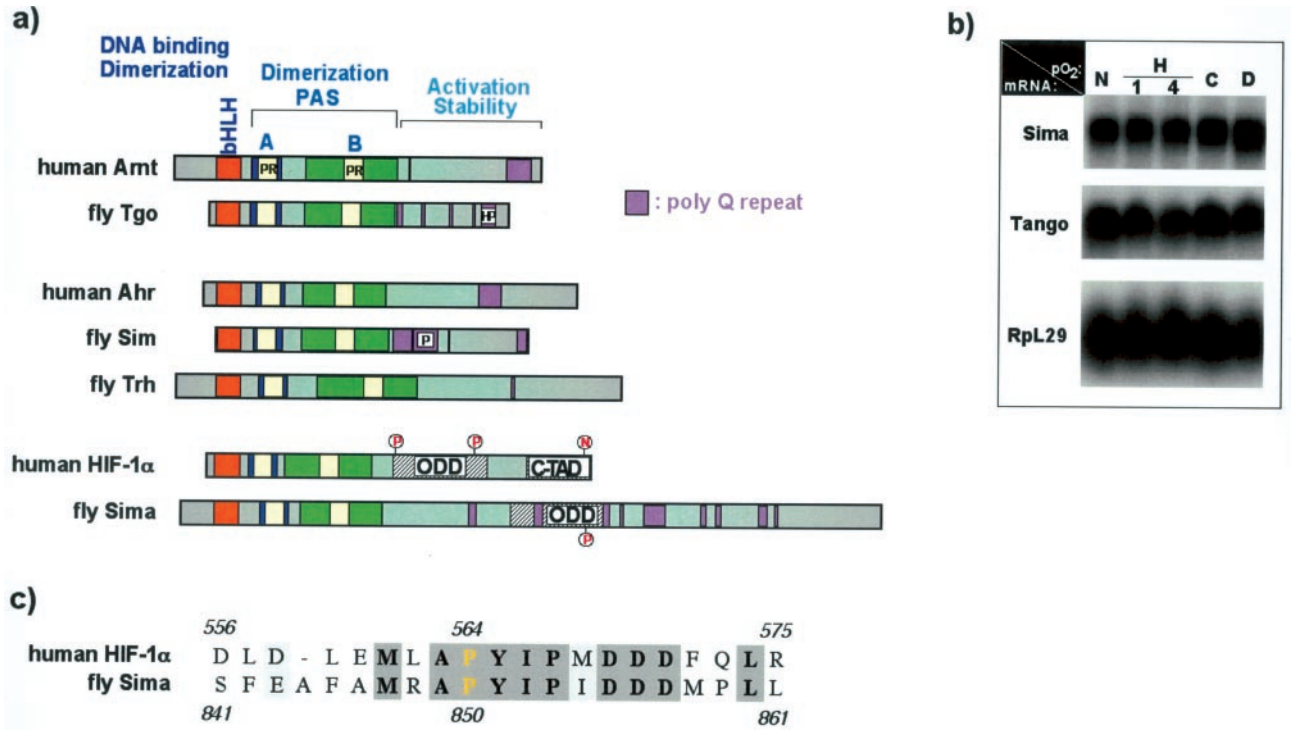

FIG. 1. **Sima and Tango are *Drosophila* candidate HIFα and HIFβ homologs.** *a*, human and *Drosophila* bHLH/PAS proteins of HIFβ (*upper*), α-like (*middle*), and HIFα (*lower*) subunits (graphics adopted, with permission, from Dr. S. Crews). The functionally important regions are as follows: the bHLH region (*orange*) with the basic region (for DNA binding) and the helix-loop-helix region (protein dimerization); the PAS A (*blue*) and PAS B (*green*) repeats (protein dimerization); polyglutamine (*poly Q*) repeats (*purple*; protein stability); the ODD (normoxic instability); C-terminal transactivation domain (*C-TAD*; interaction with coactivator proteins); and proven/potential hydroxylation residues (*P* and *N*; *circled*). *Ahr*, aryl hydrocarbon receptor. *b*, Northern blots of Sima (FlyBase ID FBgn0015542; *upper panel*), Tango (ID FBgn0015014; *middle panel*), and RpL29 (loading control; ID FBgn0016726; lower panel) mRNAs in response to 16-h exposure to normoxia (*N*), hypoxia at 1% oxygen (*H-1*), and hypoxia at 4% oxygen (*H-4*) as well as to treatment with cobalt (*C*; 100 μM $CoCl_2$) and desferrioxamine (*D*; 100 μM). *c*, alignment of human HIF-1α (residues 556–575) and *Drosophila* Sima (residues 841–861) destruction boxes. *Dark-gray boxes* indicate amino acid identities; *light-gray boxes* indicate conservative substitutions; and *gold boxes* indicate proven (Pro^{564} in human HIF-1α) or potential (Pro^{850} in Sima) proline hydroxylation targets.

to normoxic levels), establishing it to be a hypoxic, rather than anoxic, response (Fig. 2*c*). In comparison with the *in vivo* transcriptional activity of *Drosophila* HIF, with a reported pO_2 maximum at 3–5% and *sub*-normoxic activity levels at 1% oxygen (53), the DNA binding response of SL2 HIF in Fig. 2*c* was markedly shifted toward more severe O_2 reductions and even included slightly elevated anoxic HRE attachment.

Fig. 2*d* is a representative Western blot of endogenous Sima protein in SL2 nuclear extracts as a function of pO_2. In correlation with the pO_2 response of SL2 HIF activity, the abundance of Sima protein (band at 180 kDa) also peaked at 1% oxygen, declined toward both anoxia and moderate hypoxia (2.5 and 5% pO_2), and was undetectable under normoxic conditions. In addition, a 98-kDa band stained with similar intensity as the Sima 180-kDa band, but displayed linearly declining levels of abundance from anoxia to normoxia. Finally, a fainter 75-kDa band, probably representing an alternative splicing product of the *sima* gene, was detected in hypoxic but not anoxic extracts and thus might be a constituent of the faster mobility "hypoxia-only" gel shift complex noted in Fig. 2*b* (*white arrow*). In corroboration of the notion that SL2 HIF is comprised of not one, but several species derived from alternative Sima products, supershift experiments on anoxic SL2 nuclear extracts using the above anti-Sima antiserum resulted in a band split, *i.e.* the generation of *two* new bands, one being up-shifted and the other being down-shifted in comparison with the single original complex (data not shown). Taken together, the correlation between the pO_2 dependence of HIF activity and Sima stability, both showing maxima at 1% oxygen, strongly suggests that Sima acts as a functional HIFα homolog in hypoxic SL2 cells.

Although a few hypoxia-responsive fly genes have been reported (see Ref. 72 for summary), we have very limited understanding of the biological scope of *Drosophila* HIF or any other invertebrate HIF. As a first step toward this goal, we conducted a genome-wide computational survey for potential HIF target genes in both *Drosophila* and *C. elegans* as characterized by the presence of reportedly functional HRE sequences within 600 nucleotides upstream from start codons and downstream from stop codons (72). One of the genes we retrieved as a multi-HRE-flanked ORF was *glob1*, the recently discovered (73) single-copy gene for *Drosophila* globin that generates a high O_2 affinity (P_{50} ~ 0.1–0.2 torr) hemoglobin in association with the tracheal system and the fat body of fly embryos, larvae, and adults (74). Fig. 3*a* shows a diagram of the globin gene, including TATA box-like transcription start sites and potential HIF-binding HREs in 5′- and 3′-flanks as well as the coding region. At least four different globin transcripts from two different promoters are produced *in vivo* (74). All four mRNAs share the same coding region (exons 1–3) (Fig. 3*a*) and 3′-UTRs, but differ in their 5′-ends. Fly embryos express two globin transcripts, termed A (predicted ~1.0-kb size) and C (predicted ~1.3-kb size), from different promoters upstream of a respective 5′-UTR exon (Fig. 3*a*, *hatched boxes* labeled *5′A* and *5′C*, respectively) (74).

The wealth of flanking HREs, together with the fact that expression of several other invertebrate globin genes is known to be induced under low oxygen (see accompanying article (87)), led us to evaluate, by Northern blotting and exponential phase ($RT\text{-}PCR_{exp}$), the response of globin A and C mRNAs to graded hypoxia in Schneider cells (Fig. 3*b*). To our surprise, a progressive down-regulation, rather than up-regulation, of both globin

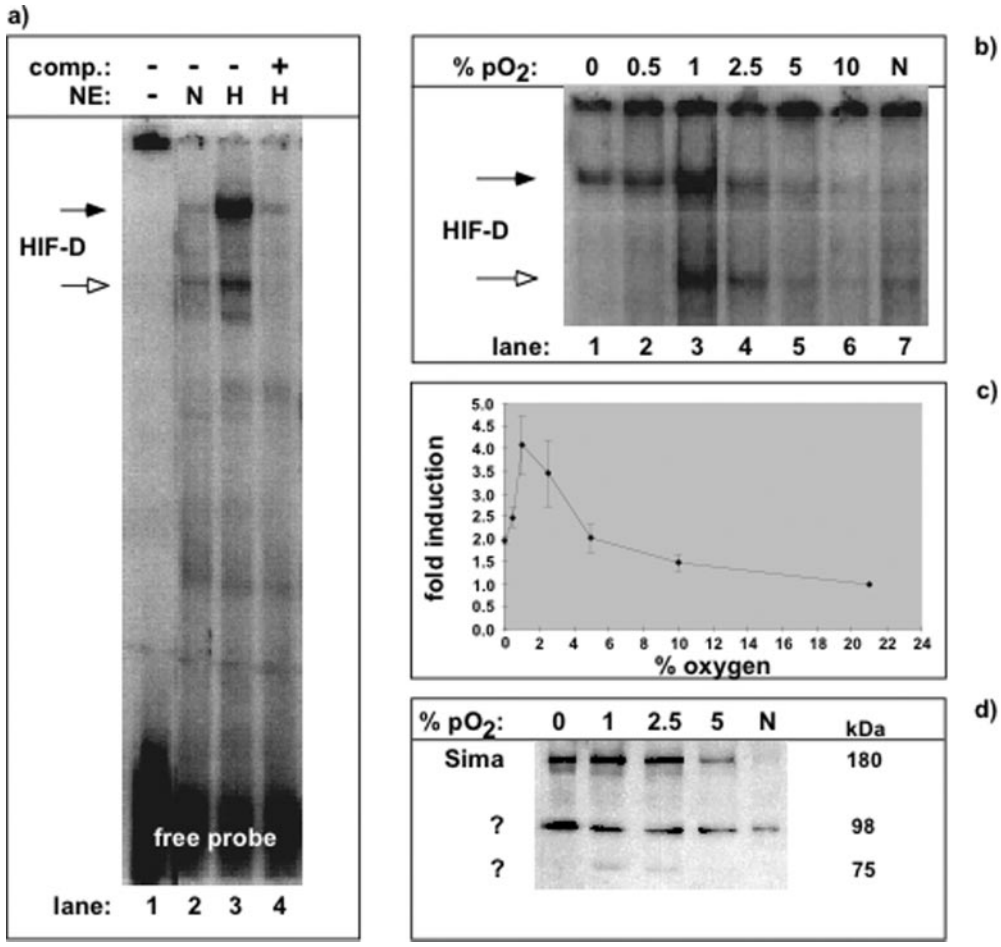

FIG. 2. **SL2 HIF activity and Sima abundance correlate with pO_2 dependence.** *a*, EMSA of SL2 HIF. Nuclear extracts (*NE*) from normoxic (*N*; 21% oxygen, 16 h) or hypoxic (*H*; 1% oxygen, 16 h) SL2 cells were incubated with the radiolabeled HRE W18 probe (see "Materials and Methods") with (*lane 4*) or without (*lanes 2* and *3*) 100-fold excess unlabeled W18 competitor (*comp.*) oligonucleotide. Free probe is shown in *lane 1*. *Drosophila* HIF (*HIF-D*) is indicated by the *black* and *white arrows* in *lane 3*. *b*, representative EMSA (only the top portion of the gel is shown) to determine the pO_2 dependence of SL2 HIF activity (*Drosophila* HIF bands indicated by the *black* and *white arrows*) in response to seven different oxygen tensions (indicated above each lane). *N*, normoxia at 21% oxygen. *c*, mean HIF activity (top complex, *black arrow* in *b*) as a function of pO_2 (*i.e.* 0, 0.5, 1, 2.5, 5, 10, *N* = 21% oxygen) obtained by phosphoimaging densitometry on three EMSA series. The mean ± S.E. of the activity for each pO_2 is shown as -fold induction relative to normoxic activity set to 1.0. *d*, Western blot of endogenous Sima protein (180 kDa) present in SL2 nuclear extracts as a function of pO_2 (indicated above each lane). Rat anti-Sima antiserum was used for Sima detection. Cross-reactivity with 98- and 75-kDa bands (?) is discussed in "Results and Discussion."

messages was observed (*Globin panels*). This suppression, already evident after 2 h at 1% oxygen, continuously increased during 16 h of hypoxia, when levels of globin transcripts declined by ~80–85% compared with normoxic controls. Completely unaffected by this hypoxia time course, Sima and Tango transcripts are presented here as loading controls. The Northern blot results (*lanes 1–5*) were in good agreement with the exponential phase RT-PCR results (*lanes 6–10*).

We next addressed whether SL2 HIF mediates the hypoxic down-regulation of globin, which would, if true, represent the first description of a trans*in*activator role conferred by an invertebrate HIF. A few cases of gene silencing are known to be *directly* triggered by human HIF signaling (75, 76). In *normoxic* mammalian cells, HIF can be fully activated by so-called hypoxia mimetics such as iron chelators (*e.g.* DFO) and transition metals (*e.g.* Co^{2+}, Ni^{2+}, and Mn^{2+} ions) (64), all of which inhibit proline hydroxylation of the α-subunit, thus stabilizing HIF even under high pO_2 (42). In contrast, and in agreement with previous reports (50), SL2 HIF was predominantly active in hypoxia, weakly so following DFO treatment of cells, and refractory to Co^{2+} ions (Fig. 3*c*), in accord with the following scheme of relative activities: hypoxia > DFO ≫ normoxia ≃ cobalt. As demonstrated in the representative Western blot in Fig. 3*c*, Sima abundance correlated with the above HIF activity ranking (*i.e.* exposure to hypoxia and DFO, but not cobalt, led to measurable Sima accumulation), once again underscoring Sima protein as the determining factor in controlling fly HIF function. The effect of these treatments on the regulation of potential HIF target genes is summarized in Fig. 3*d*. Northern blot and exponential phase RT-PCR analyses demonstrated that, compared with normoxic controls, treatment for 16 h at 1% oxygen or with 100 μM DFO caused maximal and moderate suppression of the globin A and C transcripts, respectively, whereas cobalt treatment had no significant effect on globin mRNAs (*Globin panels*). To confirm that this differential expression pattern is HIF-derived, rather than from an iron chelation/DFO-mediated inhibition of heme biosynthesis, which, in turn, could lead to moderate down-regulation of fly globin transcription, it was necessary to look for similar responses in other HRE-flanked genes encoding heme-free products. These genes included *Drosophila* lactate dehydrogenase (ImpL3, CG10160 (77), whose mRNA levels are hypoxia-inducible and, in addition, markedly suppressed by Sima RNA interference (44); CG11652, a cell cycle-regulating homolog of the human candidate tumor suppressor protein OVCA1 (78); and *Drosophila* single-copy DNA (cytosine 5)-methyltransferase (Mt2),

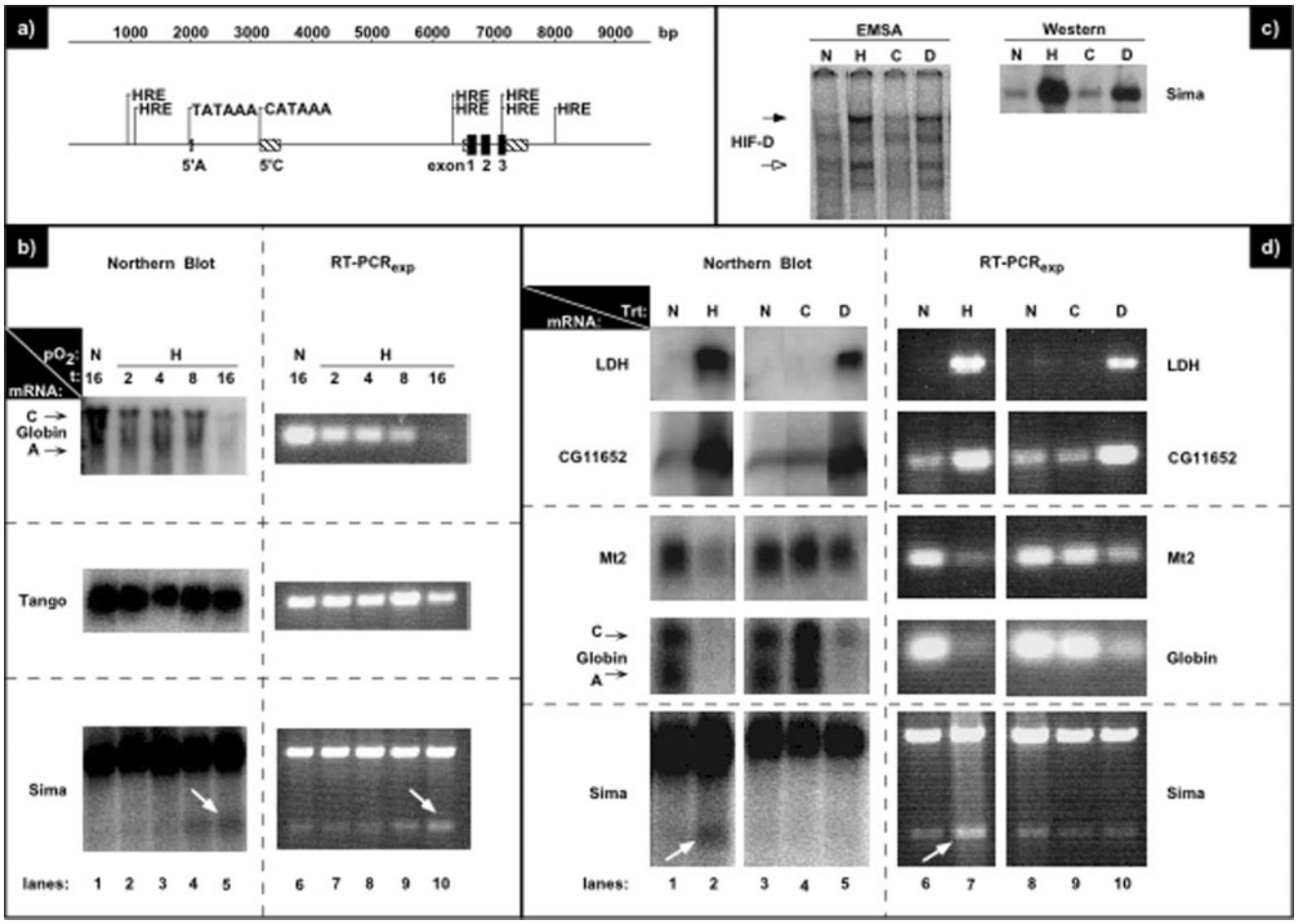

FIG. 3. **Differential HIF activity and regulation of target genes.** *a*, *Drosophila* globin gene model (*glob1*; FlyBase ID FBgn0027657) with exons (*black boxes*), 5′- and 3′-UTR DNAs (*hatched boxes*), TATA-like transcription start sites, and potential HIF-binding sites (HREs) indicated. Two globin transcripts (transcripts A and C) are expressed in fly embryos from distinct promoters upstream of the transcript A 5′-UTR exon (*5′A*) and the transcript C 5′-UTR exon (*5′C*) (74). *b*, Northern blot (*lanes 1–5*) and exponential phase RT-PCR (*RT-PCR$_{exp}$*; *lanes 6–10*) analyses of levels of SL2-expressed globin transcripts A and C (*Globin panels*), the Sima transcript (loading control; *lower panels*), and the Tango transcript (loading control; *middle panels*) following a hypoxia (*H*) time course of 2-, 4-, 8-, and 16-h exposures (*t*) to 1% oxygen in comparison with normoxic (*N*; 16 h) controls. Smaller Sima transcripts/PCR products are indicated by *white arrows*. *c*, representative EMSA and Western blot analyses of differential SL2 HIF activity (*Drosophila* HIF (*HIF-D*), *EMSA panel*, *black* and *white arrows*) and Sima stability (*Sima*, *Western panel*) in response to exposure to normoxia (*N*), 16-h hypoxia (*H*; 1% oxygen), cobalt (*C*; 100 μM $CoCl_2$), and desferrioxamine (*D*; 100 μM). *d*, Northern blot (*lanes 1–5*) and exponential phase RT-PCR (*lanes 6–10*) analyses of *Drosophila* lactate dehydrogenase (*LDH*; ImpL3; ID FBgn0001258), CG11652 (ID FBgn0036194), DNA (cytosine 5)-methyltransferase (Mt2; ID FBgn0028707), globin, and Sima (loading control) transcript levels in response to exposure to normoxic (*N*), 16-h hypoxic (*H*; 1% oxygen), cobalt (*C*; 100 μM $CoCl_2$), or desferrioxamine (*D*; 100 μM) treatment (*Trt*). Smaller Sima transcripts/PCR products are indicated by *white arrows*.

which reportedly is both necessary and sufficient for DNA methylation in fruit fly embryos (79–83).

Northern blot and RT-PCR$_{exp}$ experiments revealed similar expression changes for the lactate dehydrogenase and CG11652 transcripts (Fig. 3*d*, *LDH* and *CG11652 panels*), with maximal induction upon hypoxic treatment (~8-fold for lactate dehydrogenase and ~3-fold for CG11652), milder up-regulation triggered by DFO, and unaltered low level expression under normoxic or cobalt conditions. In contrast, Mt2 expression (*Mt2 panels*), like that of globin, was strongly inhibited by hypoxia and weakly inhibited by DFO and was not impacted by cobalt treatment compared with normoxia. As noted above (Fig. 1*b*), none of these treatments had any effect on Sima transcript levels (*Sima panels*; with the *top band* shown as a loading control). Therefore, the observed correlation between normoxia/hypoxia/cobalt/DFO-induced HIF activities or Sima abundance and the differential lactate dehydrogenase, CG11652, globin, or Mt2 expression levels demonstrates that SL2/fly HIF is able to confer both positive or negative regulations on HRE-flanked target genes.

During our assessment of Sima expression by Northern blot and RT-PCR analyses, we consistently observed one smaller band in particular (Fig. 3, *b* and *d*, *Sima panels*, *white arrows*). In striking contrast to full-length Sima mRNA, this smaller transcript was not constitutively expressed. Rather, its abundance increased linearly throughout the 2–16-h hypoxia time course (Fig. 3*b*) until, after 16 h of exposure at 1% oxygen, the levels of this transcript were 2–3-fold induced over normoxic controls (Fig. 3, *b* and *d*). Yet even at this peak abundance, the relative amount of the smaller transcript never exceeded ~13% of full-length Sima mRNA. Since the same set of PCR primers, which annealed against the start codon region of the first exon and the stop codon region of the last exon of Sima, were able to generate both the full-length (~4.5 kb) and smaller (~2.0 kb) amplicons in these competitive PCRs, both transcripts had at least these exons in common. Thus, we set out to clone and sequence both Sima amplicons in parallel.

As shown in Fig. 4*a*, sequencing of both PCR products identified them as Sima transcripts, generated by alternative splicing. The 4.5-kb PCR product corresponded to the 12-exon full-length Sima (flSima) transcript. In contrast, the 2-kb amplicon was obtained from a transcript that was composed of exons 1–7

plus exon 12. Lacking exons 8–11 in the variant mRNA agrees with the observed 2.5-kb reduction in amplicon size compared with full-length mRNA. Therefore, the smaller hypoxia-induced transcript encodes a natural ΔODD Sima splice variant (svSima), which also lacks all polyglutamine repeats, whereas it includes the entire N-terminal bHLH and PAS region (exons 1–7). In svSima, fusion of exon 7 with exon 12 resulted in a frame-shift in which only the first 19 nucleotides of exon 12 could be translated, thus generating a novel 7-amino acid C terminus (*i.e.* RMTIPKQ) (Fig. 4, *b* and *c*). Supplemental Fig. 1 presents the amino acid sequences predicted for flSima and svSima in alignment with Sima cDNA (34). From this alignment, one can see that, with few PCR or sequencing inaccuracies, flSima and svSima polypeptides are identical in sequence throughout amino acids 1–419 and that the end of the PAS region at amino acid codon 420 maps precisely to the exon 7/8 (flSima) or 7/12 (svSima) junction and thus to the end of the svSima reading frame prior to its unique 7-amino acid C terminus. Therefore, svSima mRNA is predicted to generate a 426-amino acid bHLH/PAS "mini" Sima protein that lacks the ODD and all polyglutamine motifs. Fig. 4*c* summarizes differences in the amino acid sequences between Sima cDNA, flSima, and svSima expression constructs, confirmed by DNA sequencing of at least two flSima or svSima clones. These substitutions probably represent polymorphic codons of the *sima* gene.

Obvious parallels between IPAS, the mammalian dominant-negative feedback regulator of HIF signaling (85, 86), and svSima are apparent. Both are hypoxia-induced alternative splice variants of HIFα genes that generate bHLH/PAS truncations of similar (IPAS) or identical (svSima) sequences compared with their full-length equivalents. One might expect that, being devoid of the ODD, svSima would be a constitutively stable slow turnover HIFα protein in contrast to flSima. The anti-Sima antiserum used in Fig. 2*d* was directed against amino acids 284–498, of which only amino acids 284–419 are retained in svSima, which probably explains our inability to detect endogenous svSima protein in nuclear or cytosolic extracts from SL2 cells. This conclusion is supported by the failure of this anti-Sima antiserum to detect svSima overexpressed in transfected SL2 cells (data not shown).

To explore the functional differences between flSima and svSima, both proteins were tagged and overexpressed in SL2 cells. For this purpose, the 4.5-kb flSima and 1.3-kb svSima translation frames (see "Materials and Methods") were subsequently subcloned into an insect-specific pAc5.1 expression vector, enabling the addition of C-terminal V5 epitope and poly-His tags (Fig. 4*b*). The Western blot in Fig. 5 documents, for overexpressed flSima, the expected ~180-kDa band (Fig. 2*d*) in nuclear extracts with enhanced concentration in hypoxic samples (*lanes 2* and *4*) and, for overexpressed Tango protein, a more or less constitutively stable ~83-kDa band that also predominates in nuclear extracts (*lanes 1–4*). *In vivo*, Tango protein specifically translocates from the cytosol to the nucleus only in the presence of an α-like partner protein such as Sim or Trh (54, 58, 59). To find it within the nuclei of *normoxic* SL2 cells (*lanes 1* and *3*) suggests the presence of a Tango partner protein other than endogenous Sima, Sim, or Trh (see above). In contrast, the ~55-kDa svSima band was observed exclusively in the cytosol (*lanes 6–8*). Removal of exons 8–11 apparently deleted sequences that serve as nuclear localization signals of the Sima polypeptide. The Sima exon 1–7/12 spliced mRNA thus creates a ΔODD HIFα polypeptide that also seems to be devoid of nuclear localization signals. In addition, and to our surprise, svSima protein, rather than being constitutively stable, was far more abundant in hypoxic compared with normoxic samples (*i.e. lane 5 versus lane 6* and *lane 7 versus lane 8*).

To better understand the markedly enhanced hypoxia stability of a ΔODD HIFα protein, Sima Northern blotting of SL2 cells transfected with flSima and svSima was conducted to determine whether the predominant occurrence of svSima protein under hypoxic conditions could be explained by differential oxygen-dependent stabilities of its overexpressed transcript. In these Northern analyses, we indeed found marked degradation of transfected svSima and, to a lesser extent, flSima transcripts particularly at normoxic pO_2 (data not shown). This suggests that the augmented normoxic degradation of *overexpressed* svSima mRNA might at least contribute to the seemingly greater abundance of this splice variant protein in hypoxic cells.

To further investigate the potential biological role of svSima, we carried out Northern blot analyses of candidate HIF target genes (Fig. 3*d*) following transient SL2 transfection of increasing amounts of either the pAc5.1/flSima or pAc5.1/svSima construct. As shown in Fig. 6, increasing amounts of flSima (2 and 10 μg of construct) (*lanes 3–6*) clearly enhanced the hypoxic suppression of globin and Mt2 transcripts (*Globin* and *Mt2 panels*, *lane 2 versus lane 4*, *double arrows*). At 10 μg of construct, perhaps sufficient to overcome the cells' proteolytic machinery, flSima down-regulated globin and Mt2 transcript levels even in normoxia (*lane 1 versus lane 5*, *double arrows*), providing further support that both these genes are HIF targets. In marked contrast, the svSima transcript (2 and 10 μg of construct) (*lanes 9–12*) stimulated both the normoxic (*lane 7 versus lane 11*) and hypoxic (*lane 8 versus lane 12*) expression of the *globin* and *mt2* genes (*double arrow*s) in a dose-dependent manner, thus conferring, at least in part, relief from Sima-mediated gene silencing. In support of the role of Sima as a transactivator protein in SL2 cells, the hypoxic induction of both lactate dehydrogenase and CG11652 was visibly enhanced with increasing amounts of the flSima construct (*LDH* and *CG11652 panels*, *lane 2 versus lane 6*, *double arrows*), whereas overexpression of svSima had little effect on either target (Fig. 6). Apparently, svSima functions gene-specifically and may be more effective in reversing Sima-controlled gene suppression, rather than induction, thus pointing to a selective mode of interference. Steady-state levels of the loading control transcript RpL29 were unaffected by flSima or svSima overexpression (*RpL29 panel*).

The fact that overexpressed flSima augmented both down-regulated (globin and Mt2) and up-regulated (lactate dehydrogenase and CG11652) hypoxic transcription supports the above-mentioned correlation between differential HIF activity or Sima abundance and gene expression levels (Fig. 3, *c* and *d*). From these data, it is clear, that Sima (HIF) functions gene-specifically and highly economically as a hypoxic transactivator (lactate dehydrogenase and CG11652) and trans*in*activator (globin and Mt2) complex, respectively. A similar duality in function has recently been established for human HIF and led to the proposed existence of activating *versus* silencing HIF/HRE·coactivator complexes (75, 76). The above observations document that far ranging physiological functions in *Drosophila* such as oxygen transport/scavenging (globin), DNA methylation (Mt2), glycolytic reactions (lactate dehydrogenase), and cell cycle control (CG11652) are all oxygen-dependent and impacted by fly Sima/HIF. Moreover, since transiently expressed svSima was able to antagonize HIF-driven suppression (globin and Mt2) far better than induction (lactate dehydrogenase and CG11652), the data presented in Fig. 6 suggest different susceptibilities to svSima interference of suppressive *versus* inductive HIF·coactivator complexes.

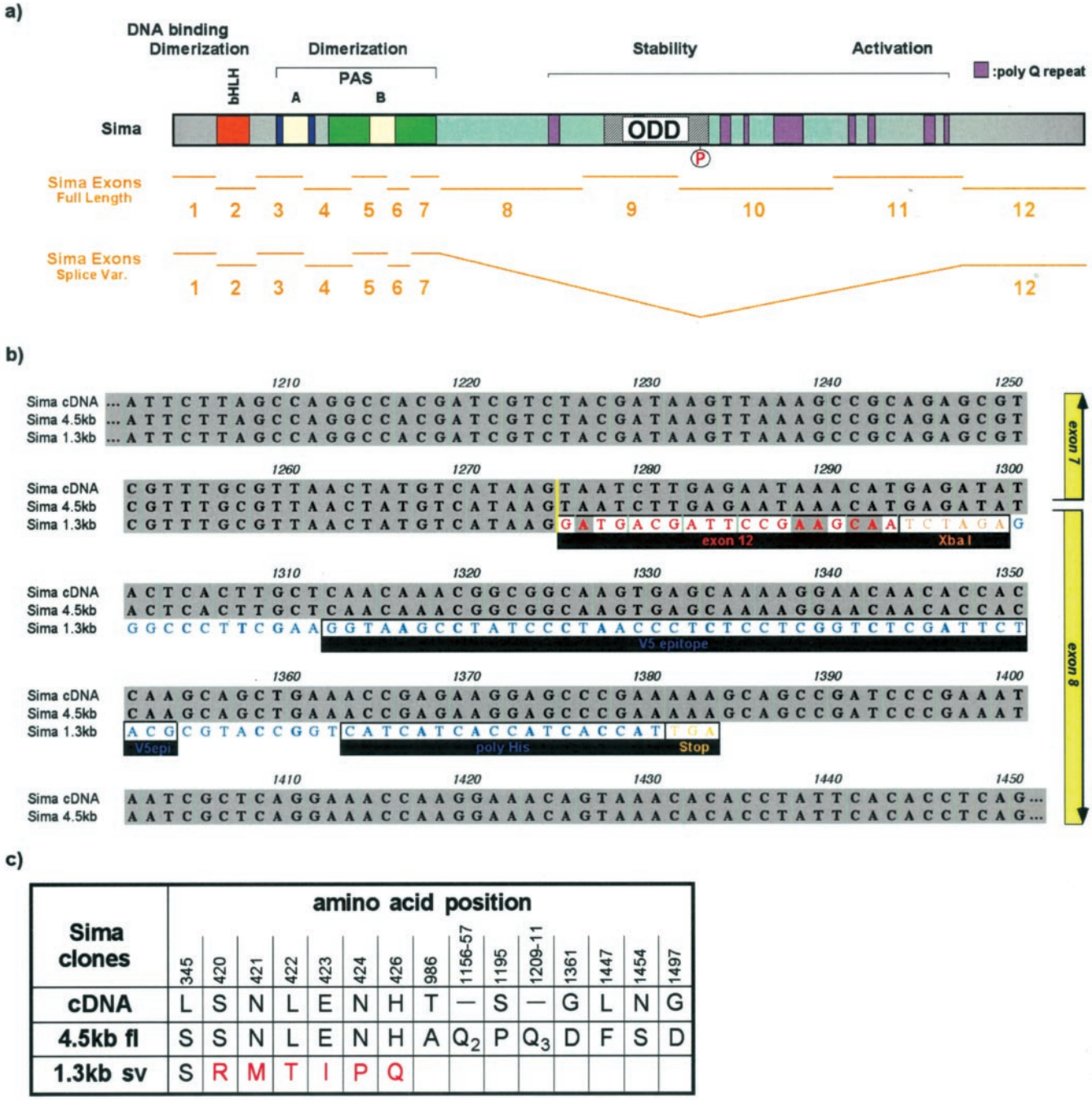

c)

Sima clones	amino acid position														
	345	420	421	422	423	424	426	986	1156-57	1195	1209-11	1361	1447	1454	1497
cDNA	L	S	N	L	E	N	H	T	—	S	—	G	L	N	G
4.5kb fl	S	S	N	L	E	N	H	A	Q_2	P	Q_3	D	F	S	D
1.3kb sv	S	R	M	T	I	P	Q								

FIG. 4. **svSima is a natural ΔODD Sima splice variant.** *a*, exon composition of flSima (exons 1–12; *middle*) and svSima (exons 1–7/12; *lower*) transcripts in scale with the Sima protein model (*upper*), with the functionally relevant regions (*i.e.* bHLH, PAS, ODD, and polyglutamine repeats (*poly Q*); see Fig. 1*a* for details) highlighted. *b*, alignment of the exon 7/8 junction in Sima cDNA (*upper*) (34) and the 4.5-kb amplicon of flSima (*Sima 4.5kb*; *middle*) in comparison with the exon 7/12 junction in the 1.3-kb svSima translation frame (*Sima 1.3kb*; *lower*). Identical sequences (*gray backgrounds*), amino acid codons (*light-blue lines*), and phase 2 exon 7/8 (Sima cDNA and flSima) and 7/12 (svSima) junctions (*yellow line*) are indicated in the nucleotide sequence alignment. In the *Sima 1.3kb sequence*, exon 12 (*red*), the XbaI restriction site (*brown*), and pAc5.1 expression vector DNA (*blue*), including the V5 epitope, poly-His motif, and vector-provided stop codon (*gold*) are indicated. *c*, summary of all amino acid differences between Sima cDNA (*upper*) (34) and the full-length (4.5 kbfl; *middle*) and splice variant (1.3 kbsv; *lower*) expression constructs. cDNA ↔ flSima or svSima substitutions were confirmed in at least two independent Sima clones and, therefore, probably represent polymorphic codons of the *sima* gene. Note the increased substitution frequency toward C termini between Sima cDNA and flSima polypeptides, particularly within exon 12 (positions 1361, 1447, 1454, and 1497), possibly in reflection of region dispensability for some Sima protein products (svSima). The unique svSima C terminus is shown in *red*. Q_2 and Q_3 indicated two and three consecutive glutamine mismatches, respectively.

For additional studies of the functional differences between fly HIF proteins, SL2 cells were cotransfected with HRE-luciferase reporter constructs along with flSima, svSima, and Tango expression plasmids and incubated under normoxic or hypoxic pO_2. The luciferase reporter contained a triple-HRE portion of the promoter of the hypoxia-inducible hemoglobin-2 gene from the freshwater crustacean *Daphnia magna* that was cloned upstream of the luciferase gene in the pGL3-Basic plasmid (Fig. 7, *inset*). Two of these three HREs are able to bind human, *Drosophila*, or *Daphnia* HIF proteins (see accompanying article (87)). As shown in Fig. 7 (*sections 1–3*), all negative controls (*i.e.* plasmid-free and insert-free reporter plasmid transfections, with and without cotransfected flSima) failed to show any significant luciferase activities. Similarly, transfec-

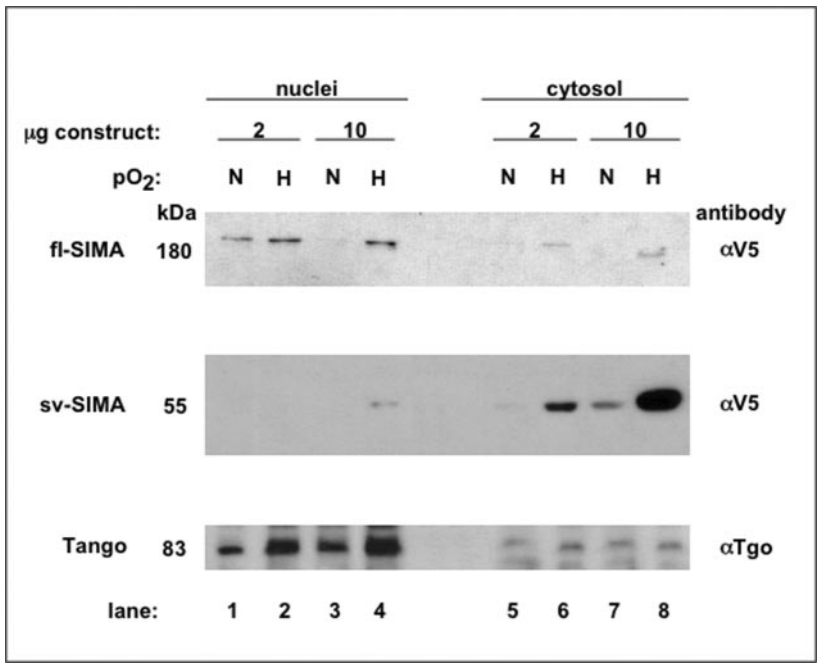

FIG. 5. **flSima localizes in the nucleus and svSima in the cytosol.** Shown are the results from Western blot detection of overexpressed flSima (180-kDa band; *upper panel*), svSima (55-kDa band; *middle panel*), and Tango (83-kDa band; *lower panel*) in nuclear (*nuclei*) and cytosolic (*cytosol*) fractions of normoxic (*N*) and hypoxic (*H*; 1% oxygen, 16 h) SL2 cells. The microgram amounts of the pAc5 expression construct used in each transfection are indicated. The antibodies used were the anti-V5 monoclonal antibody for V5 epitope-tagged flSima and svSima proteins and the anti-Tgo monoclonal antibody for Tango protein.

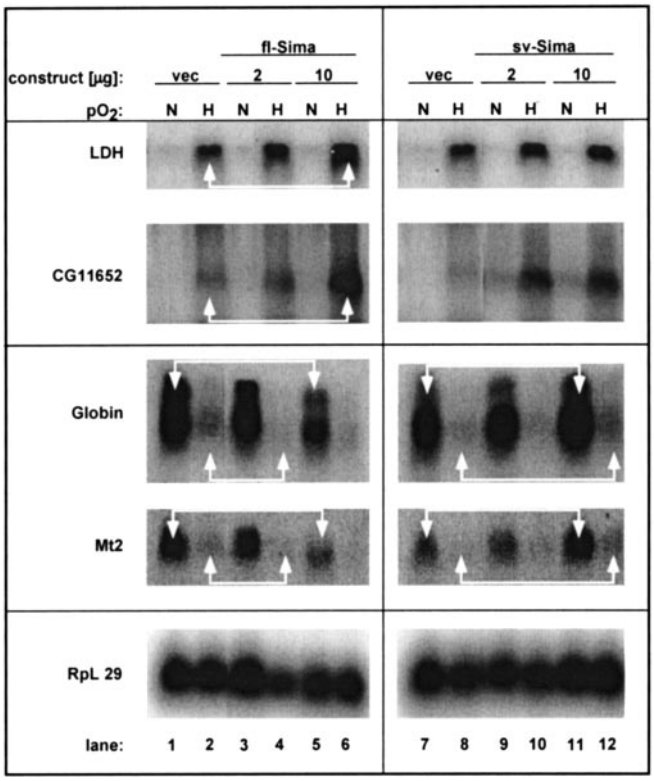

FIG. 6. **Agonistic and antagonistic effects of flSima or svSima overexpression on target genes.** Shown are the results from Northern blot screening of lactate dehydrogenase (*LDH*; ImpL3), CG11652, globin, Mt2, and RpL29 (loading control) in response to mock (*vec*; 20 µg of pAc5.1 vector), flSima (2 and 10 µg of construct; filled to 20 µg of plasmid with pAc5.1), or svSima (2 and 10 µg of construct; filled to 20 µg of plasmid with pAc5.1) transfection. 32 h post-transfection, SL2 transfectants were exposed to normoxic (*N*) or hypoxic (*H*; 1% oxygen) pO_2 values for 16 h. *Double arrows* highlight the most important alterations in mRNA levels of candidate HIF target genes (discussed in "Results and Discussion").

tion of the HRE-reporter alone yielded only base-line activation of the luciferase gene, suggesting that low levels of active endogenous HIF complexes are present in the SL2 batches used for these transfections (*section 4*). However, cotransfecting the HRE-reporter with the flSima construct alone (*section 6a*) transactivated specifically the hypoxic reporter expression and resulted in an ~8.5-fold induction under 1% oxygen, in good agreement with previous Sima-Gal4 fusion construct UAS/luciferase assays in Hep3B cells (52) and with the predominant occurrence of the protein in hypoxic nuclei of SL2 cells (Fig. 5). In marked contrast, neither Tango (*section 7a*) nor svSima (*section 5*) cotransfections were able to stimulate the reporter under any (normoxic or hypoxic) condition above the vector controls used. Since Sima is known to interact only with either Tango or human ARNT to generate functional HIF complexes (36, 52) and since no evidence for Sima·Sima homodimers has been reported, it is likely that the hypoxic induction of reporters in response to Sima cotransfections (Fig. 7) (52) depends on heterodimers formed between overexpressed Sima and endogenous Tango/ARNT polypeptides. Failure of overexpressed Tango to activate the HRE-reporter also indicates that endogenous Sima is limiting for HIF-driven gene regulation. The failure of svSima to confer stimulated luciferase expression agrees well with its exclusive cytosolic residence (Fig. 5) and its deletion of a transactivation domain within the ODD. In comparison with flSima alone, flSima+Tango (*i.e.* HIF) double transfections (*section 8a*) resulted in no significant change in hypoxic transcription, which again supports the presence of excess endogenous Tango in SL2 cells.

To further assess the influence of svSima on HIF function, we titrated the activity of the HRE-reporter mediated by flSima (Fig. 7, *section 6b*), Tango (*section 7b*), and flSima+Tango (*section 8b*) by cotransfection with increasing amounts of the svSima expression construct. svSima decreased Sima- and Sima+Tango-driven reporter expression in a dose-dependent manner while maintaining their hypoxic induction across the whole range of svSima concentrations used. Note, however, that low doses of the svSima expression construct (*i.e.* 0.65 µg in *sections 6b* and *8b*) primarily diminished hypoxic, rather than normoxic, reporter activities, in support of a predominantly hypoxic role of the splice variant product.

This induction-maintaining antagonism of Sima (Fig. 7, *section 6*) or HIF (*section 8*) function by svSima suggests that Tango, *i.e.* the HIF constitutive component, is captured by the splice variant, thus forming an unproductive cytosolic heterodimer at the expense of flSima·Tango complexes. This hy-

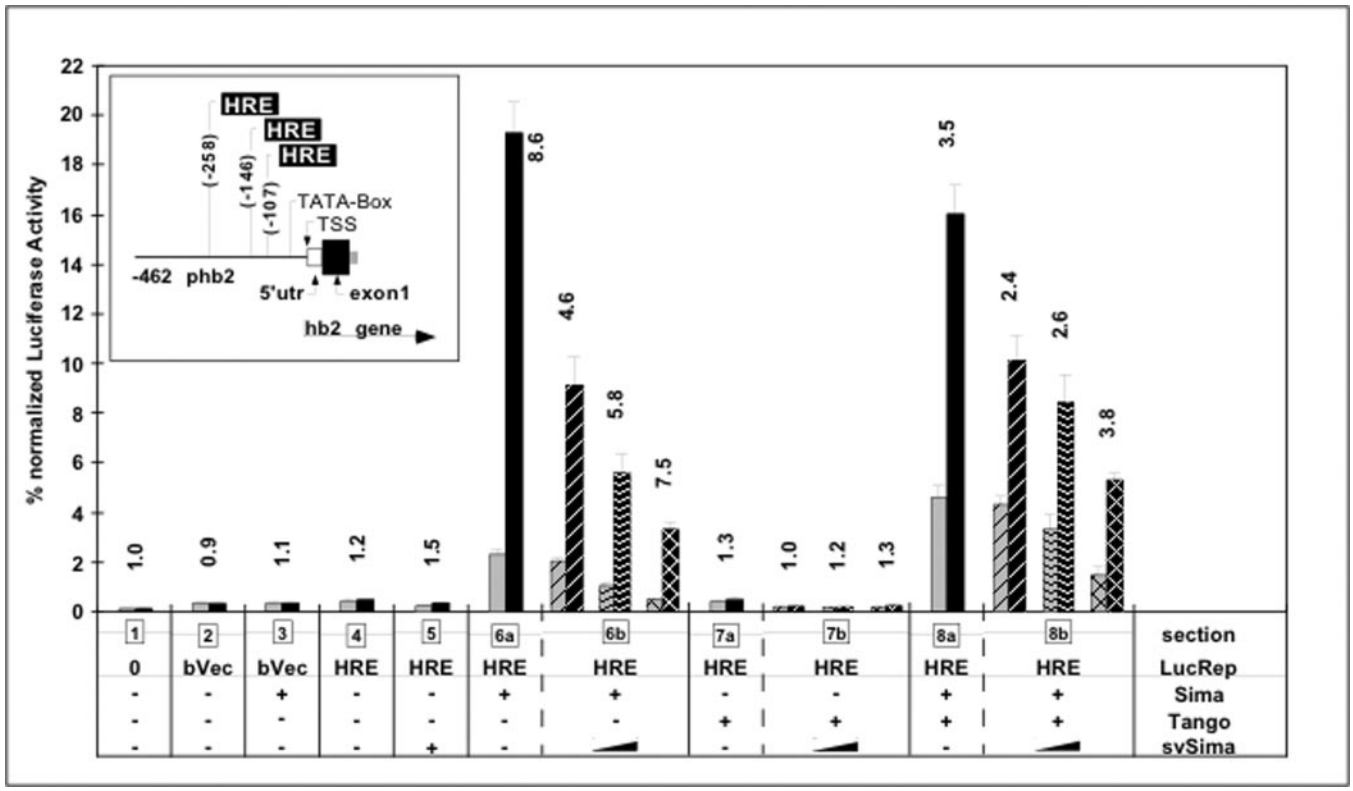

FIG. 7. **Constitutive inhibition of Sima and HIF function by increasing expression of svSima.** Shown are the results from the luciferase reporter assay of SL2 cells cotransfected with flSima (*Sima*), Tango, or svSima expression constructs and HRE-luciferase reporter plasmids (*LucRep*) as depicted underneath the graphics. Percentages of mean (±S.E.) and β-galactosidase normalized normoxic (*gray bars*) and hypoxic (*black bars*) luciferase activities are shown (n = six cotransfections). *Sections 1–3* show negative controls (plasmid-free transfection (*0*) and insert-free pGL3-Basic luciferase vector-only transfection (*bVec*)) without (−; *section 2*) and with (+; *section 3*) flSima cotransfection. For *Sections 4–8*, *LucRep* indicates the −462 base deletion product of the *Daphnia* triple-HRE *hb2* promoter (*inset*, *−462 phb2*) upstream of the pGL3-Basic vector luciferase gene used as the HRE-luciferase reporter (*HRE*). *Sections 4–8* show HRE-luciferase cotransfections with various HIF expression constructs. *Section 4*, no HIF cotransfection (HRE-luciferase reporter only); *section 5*, HRE-luciferase reporter + svSima; *section 6a*, HRE-luciferase reporter + flSima; *section 7a*, HRE-luciferase reporter + Tango; *section 8a*, HRE-luciferase reporter + flSima and Tango; sections *6b–8b*, HRE-luciferase reporter + flSima, Tango, and flSima/Tango (0.25 μg), respectively, and svSima in increasing amounts (+0.65 (*hatched*), +2.0 (*waved*), and +6.5 μg (*crossed bars*)). Hypoxic -fold inductions (*i.e. black/gray bar* mean luciferase activity ratios) are shown above each transfection. *TSS*, transcription start site.

pothesis is in line with results from earlier yeast two-hybrid analyses reporting avid and specific interactions between Tango and the N-terminal portion of Sima used as the bait construct (*i.e.* Sima amino acids 32–488 (36); compare with Sima amino acids 1–419 present in svSima). On the other hand, mammalian IPAS forms abortive complexes in physical contact with HIFα proteins and consequentially reduces hypoxic induction dose-dependently in similar transfection titration experiments (85).

On the basis of our svSima overexpression results, we propose a model in which a cytosolic *sima* gene splice variant (svSima) serves, specifically under hypoxic conditions, to control access of Tango protein to flSima and other α-like bHLH/PAS partners in *Drosophila* cells: when svSima is present at low levels (normoxia), Tango can "freely" bind to partner proteins (*e.g.* Dys) and translocate into the nucleus. Once its levels begin to increase (hypoxia), svSima can more effectively sequester Tango into the cytosol and keep it away from nuclear partners (Sima and Dys), thus serving to regulate the relative activities of Tango complexes and eventually even terminating Sima/HIF-controlled gene regulation. Therefore, the *sima* gene expresses its own agonistic and antagonistic or regulatory protein products.

Further work is needed to extend the findings reported here to *in vivo* models to assess potential tissue-specific expression of svSima protein as has been reported for IPAS (85) and changes in svSima production at different developmental stages. These studies will help to determine whether svSima is involved in the fine-tuning of HIF-dependent gene expression. It will also be of interest to work out the mechanism responsible for the oxygen-dependent splicing of Sima transcripts. Finally, we need to assess the quantitative levels of the different α-like bHLH/PAS proteins in cells and tissues as well as their relative affinities for Tango to elucidate the impact of regulatory factors such as svSima on various Tango complexes and on bHLH/PAS protein-mediated signaling pathways.

Acknowledgments—We gratefully acknowledge Drs. A. Michelson and N. Perrimon for the gift of SL2 cultures and Dr. S. Crews for the gift of anti-Tango antibody and Tango expression constructs. We also thank Dr. S. Crews for invaluable feedback throughout this project.

REFERENCES

1. Bunn, H. F., and Poyton, R. O. (1996) *Physiol. Rev.* **76,** 839–885
2. Hochachka, P. W., Buck, L. T., Doll, C. J., and Land, S. C. (1996) *Proc. Natl. Acad. Sci. U. S. A.* **93,** 9493–9498
3. Hochachka, P. W. (1986) *Science* **231,** 234–241
4. Wegener, G. (1988) in *Oxygen Sensing in Tissues* (Acker, H., ed) pp. 13–35, Springer-Verlag, Berlin
5. Wegener, G. (1993) in *Surviving Hypoxia: Mechanisms of Control and Adaptation* (Hochachka, P. W., Lutz, P. L., Sick, T., Rosenthal, M., and van den Thillart, G., eds) pp. 417–434, CRC Press LLC, Boca Raton, FL
6. Haddad, G. G. (2000) *J. Appl. Physiol.* **88,** 1481–1487
7. Csik, L. (1939) *Z. Vgl. Physiol.* **27,** 304–310
8. Chadwick, L. E., and Gilmour, D. (1940) *Physiol. Zool.* **13,** 398–410
9. Keister, M., and Buck, J. (1974) in *The Physiology of Insecta* (Rockstein, M., ed) 2nd Ed., Vol. 6, pp. 469–509, Academic Press, Inc., New York
10. Loudon, C. (1988) *J. Insect Physiol.* **34,** 97–103
11. Wingrove, J. A., and O'Farrell, P. H. (1999) *Cell* **98,** 105–114
12. Krishnan, S. N., Sun, Y.-A., Mohsenin, A., Wyman, R. J., and Haddad, G. G. (1997) *J. Insect Physiol.* **43,** 203–210

13. Grieshaber, M. K., Hardewig, I., Kreutzer, U., and Pörtner, H.-O. (1994) *Rev. Physiol. Biochem. Pharmacol.* **125,** 43–147
14. Foe, V. E., and Alberts, B. M. (1985) *J. Cell Biol.* **100,** 1623–1636
15. Douglas, R. M., Xu, T., and Haddad, G. G. (2001) *Amer. J. Physiol.* **280,** R1555–1563
16. DiGregorio, P. J., Ubersax, J. A., and O'Farrell, P. H. (2001) *J. Biol. Chem.* **276,** 1930–1937
17. Wigglesworth, V. B. (1954) *Q. J. Microsc. Sci.* **95,** 115–137
18. Locke, M. (1958) *Q. J. Microsc. Sci.* **99,** 373–391
19. Jarecki, J., Johnson, E., and Krasnow, M. A. (1999) *Cell* **99,** 211–220
20. Metzger, R. J., and Krasnow, M. A. (1999) *Science* **284,** 1635–1639
21. Klagsbrun, M., Knighton, D., and Folkman, J. (1976) *Cancer Res.* **36,** 110–114
22. Shweiki, D., Itin, A., Soffer, D., and Keshet, E. (1992) *Nature* **359,** 843–845
23. Levy, A., Levy, N., Wegner, S., and Goldberg, M. (1995) *J. Biol. Chem.* **270,** 13333–13340
24. Maxwell, P. H., Pugh, C. W., and Ratcliffe, P. J. (1993) *Proc. Natl. Acad. Sci. U. S. A.* **90,** 2423–2427
25. Guang, L. W., and Semenza, G. L. (1993) *Proc. Natl. Acad. Sci. U. S. A.* **90,** 4304–4308
26. Guillemin, K., and Krasnow, M. A. (1997) *Cell* **89,** 9–12
27. Crews, S. (1998) *Genes Dev.* **12,** 607–620
28. Ledent, V., and Vervoort, M. (2001) *Genome Res.* **11,** 754–770
29. Peyrefitte, S., Kahn, D., and Haenlin, M. (2001) *Mech. Dev.* **104,** 99–104
30. Wang, G. L., and Semenza, G. L. (1995) *J. Biol. Chem.* **270,** 1230–1237
31. Wang, G. L., Jiang, B. H., Rue, E. A., and Semenza, G. L. (1995) *Proc. Natl. Acad. Sci. U. S. A.* **92,** 5510–5514
32. Powell-Coffman, J. A., Bradfield, C. A., and Wood, W. B. (1998) *Proc. Natl. Acad. Sci. U. S. A.* **95,** 2844–2849
33. Jiang, H., Guo, R., and Powell-Coffman, J. A. (2001) *Proc. Natl. Acad. Sci. U. S. A.* **14,** 7916–7921
34. Nambu, J. R., Chen, W., Hu, S., and Crews, S. T. (1996) *Gene* (*Amst.*) **172,** 249–254
35. Ohshiro, T., and Saigo, K. (1997) *Development* (*Camb.*) **124,** 3975–3986
36. Sonnenfeld, M., Ward, M., Nystrom, G., Mosher, J., Stahl, S., and Crews, S. (1997) *Development* (*Camb.*) **124,** 4571–4582
37. Ma, E., and Haddad, G. G. (1999) *Mol. Brain Res.* **73,** 11–16
38. Ebert, B. L., and Bunn, H. F. (1999) *Blood* **94,** 1864–1877
39. Wenger, R. H. (2000) *J. Exp. Biol.* **203,** 1253–1263
40. Wenger, R. H., and Gassmann, M. (1997) *Biol. Chem.* **378,** 1–8
41. Huang, L. E., and Bunn, H. F. (2003) *J. Biol. Chem.* **278,** 19575–19578
42. Epstein, A. C. R., Gleadle, J. M., McNeill, L. A., Hewitson, K. S., O'Rourke, J., Mole, D. R., Mukherji, M., Metzen, E., Wilson, M. I., Dhanda, A., Tian, Y., Masson, N., Hamilton, D. L., Jaakola, P., Barstead, R., Hodgkin, J., Maxwell, P. H., Pugh, C. W., Schofield. C. J., and Ratcliffe, P. J. (2001) *Cell* **107,** 43–54
43. Semenza, G. L. (2001) *Cell* **107,** 1–3
44. Bruick, R. K., and McKnight, S. L. (2001) *Science* **294,** 1337–1340
45. Huang, L. E., Gu, J., Schau, M., and Bunn, H. F. (1998) *Proc. Natl. Acad. Sci. U. S. A.* **95,** 7987–7992
46. Salceda, S., and Caro, J. (1997) *J. Biol. Chem.* **272,** 22642–22647
47. Maxwell, P. H., Wiesener, M. S., Chang, G. W., Clifford, S. C., Vaux, E. C., Cockman, M. E., Wykoff, C. C., Pugh, C. W., Maher, E. R., and Ratcliffe, P. J. (1999) *Nature* **399,** 271–275
48. Cockman, M. E., Masson, N., Mole, D. R., Jaakola, P., Change, G. W., Clifford, S. C., Maher, E. R., Pugh, C. W., Ratcliffe, P. J., and Maxwell, P.H. (2000) *J. Biol. Chem.* **275,** 25733–25741
49. Tanimoto, K., Makino, Y., Pereira, T., and Poellinger. L. (2000) *EMBO J.* **19,** 4298–4309
50. Nagao, M., Ebert, B. L., Ratcliffe, P. J., and Pugh, C. W. (1996) *FEBS Lett.* **387,** 161–166
51. Srinivas, V., Zhang, L.-P., Zhu, X.-H., and Caro, J. (1999) *Biochem. Biophys. Res. Commun.* **260,** 557–561
52. Bacon, N. C. M., Wappner, P., O'Rourke, J. F., Bartlett, S. M., Shilo, B.-Z., Pugh, C. W., and Ratcliffe, P. J. (1998) *Biochem. Biophys. Res. Commun.* **249,** 811–816N. C. M.
53. Lavista-Llanos, S., Centanin, L., Irisarri, M., Russo, D. M., Gleadle, J. M., Bocca, S. N., Muzzopappa, M., Ratcliffe, P. J., and Wappner, P. (2002) *Mol. Cell. Biol.* **22,** 6842–6853
54. Ward, M. P., Mosher, J. T., and Crews, S. T. (1998) *Development* (*Camb.*) **125,** 1599–1608
55. Nambu, J. R., Lewis, J. O., Wharton, K. A., Jr., and Crews, S. T. (1991) *Cell* **67,** 1157–1167
56. Isaac, D. D., and Andrew, D. J. (1996) *Genes Dev.* **10,** 103–117
57. Wilk, R., Weizman, I., and Shilo, B.-Z. (1996) *Genes Dev.* **10,** 93–102
58. Emmons, R. B., Duncan, D., Estes, P. A., Kiefel, P., Mosher, J. T., Sonnenfeld, M., Ward, M. P., Duncan, I., and Crews, S. T. (1999) *Development* (*Camb.*) **126,** 3937–3945
59. Jiang, L., and Crews, S. T. (2003) *Mol. Cell. Biol.* **23,** 5625–5637
60. Wharton, K. A., Jr., Franks, R. G., Kasai, Y., and Crews, S. T. (1994) *Development* (*Camb.*) **120,** 3563–3569
61. Denison, M. S., Fisher, J. M., and Whitlock, J. P., Jr. (1988) *J. Biol. Chem.* **263,** 17221–17224
62. Hankinson, O. (1995) *Annu. Rev. Pharmacol. Toxicol.* **35,** 307–340
63. Schneider, I. (1972) *J. Embryol. Exp. Morphol.* **27,** 353–365
64. Goldberg, M. A., Dunning, S. P., and Bunn, H. F. (1988) *Science* **242,** 1412–1415
65. Long, E. O., and Dawid, I. B. (1980) *J. Mol. Biol.* **138,** 873–878
66. Bell, J., Neilson, L., and Pellegrini, M. (1988) *Mol. Cell. Biol.* **8,** 91–95
67. Semenza, G. L., and Wang, G. L. (1992) *Mol. Cell. Biol.* **12,** 5447–5454
68. Chung, Y.-T., and Keller, E. B. (1990) *Mol. Cell. Biol.* **10,** 6172–6180
69. Southern, J. A., Young, D. F., Heaney, F., Baumgärtner, W. K., and Randall, R. E. (1991) *J. Gen. Virol.* **72,** 1551–1557
70. Graham, F. L., and van der Eb, A. J. (1973) *Virology* **52,** 456–467
71. Wigler, M., Pellicer, A., Silverstein, S., Axel, R., Urlaub, G., and Chasin, L. (1979) *Proc. Natl. Acad. Sci. U. S. A.* **76,** 1373–1376
72. Gorr, T. A., Cahn, J. D., Hradecky, P., and Bunn, H. F. (2003) in *Oxygen Sensing: Responses and Adaptation to Hypoxia* (Lahiri, S., Semenza, G. L., and Prabhakar, N. R., eds) pp. 175–199, Marcel Dekker, Inc., New York
73. Burmester, T., and Hankeln, T. (1999) *Mol. Biol. Evol.* **16,** 1809–1811
74. Hankeln, T., Jaenicke, V., Kiger, L., Dewilde, S., Ungerechts, G., Schmidt, M., Urban, J., Marden, M. C., Moens, L., and Burmester, T. (2002) *J. Biol. Chem.* **277,** 29012–29017
75. Narravula, S., and Colgan, S. P. (2001) *J. Immunol.* **166,** 7543–7548; Correction (2002) *J. Immunol.* **168,** 3113
76. Mazure, N. M., Chauvet, C., Bois-Joyeux, B., Bernard, M.-A., Nacer-Chérif, H., and Danan, J.-L. (2002) *Cancer Res.* **62,** 1158–1165
77. Abu-Shumays, R. L., and Fristrom, J. W. (1997) *Dev. Genet.* **20,** 11–22
78. Bruening, W., Prowse, A. H., Schultz, D. C., Holgado-Madruga, M., Wong, A., and Godwin, A. K. (1999) *Cancer Res.* **59,** 4973–4983
79. Tweedie, S., Ng, H.-H., Barlow, A. L., Turner, B. M., Hendrich, B., and Bird, A. (1999) *Nat. Genet.* **23,** 389–390
80. Lyko, F., Ramsahoye, B. H., and Jaenisch, R. (2000) *Nature* **408,** 538–540
81. Gowher, H., Leismann, O., and Jeltsch, A. (2000) *EMBO J.* **19,** 6918–6923
82. Lyko, F. (2001) *Trends Genet.* **17,** 169–172
83. Kunert, N., Marhold, J., Stanke, J., Stach, D., and Lyko, F. (2003) *Development* (*Camb.*) **130,** 5083–5090
84. Taylor, B. L., and Zhulin, I. B. (1999) *Microbiol. Mol. Biol. Rev.* **63,** 479–506
85. Makino, Y., Cao, R., Svensson, K., Bertilsson, G., Asman, M., Tanaka, H., Cao, Y., Berkenstam, A., and Poellinger, L. (2001) *Nature* **414,** 550–554
86. Makino, Y., Kanopka, A., Wilson, W. J., Tanaka, H., and Poellinger, L. (2002) *J. Biol. Chem.* **277,** 32405–32408
87. Gorr, T. A., Cahn, J. D., Yamagata, H., and Bunn, H. F. (2004) *J. Biol. Chem.* **279,** 36038–36047